2010

Observational studies on association between eastward equatorial jet and Indian Ocean dipole

Chu, Peter C.

Journal of Oceanography, Vol. 66, pp. 429 to 434, 2010

Short Contribution

Observational Studies on Association between Eastward Equatorial Jet and Indian Ocean Dipole

PETER C. CHU*

Department of Oceanography, Naval Postgraduate School, Monterey, CA 93493, U.S.A.

(Received 27 February 2009; in revised form 12 January 2010; accepted 20 January 2010)

Association between weakening/strengthening of the eastward equatorial jet (EEJ) in both seasons and the Indian Ocean dipole (IOD) was investigated using two independent observational datasets (October 1992 to September 2007): (a) the dipole mode index $I(t)$ and (b) the 5-day Ocean Surface Current Analyses-Realtime (OSCAR) obtained from satellite altimetry and scatterometer data, which has strong seasonal variability, with the EEJ occurrence in spring and fall, shown from the time-longitude cross-section of equatorial zonal velocity (1°S–1°N). The association is detected in two ways. First, time series of averaged zonal velocity over (1°S–1°N, 42°E–100°E) $U(t)$ shows a close association to the dipole mode index: positive IOD events (1994, 1997, 2006) correspond to negative U (westward equatorial current), and negative IOD events (1994, 1995, 1999, 2005) correspond to positive U (eastward equatorial current). Second, the EEJ weakening/strengthening is represented by the streamfunction anomaly relative to its climatological monthly mean fields. The streamfunction anomaly is further analyzed using the empirical orthogonal function (EOF) method. The first EOF mode accounts for 55% of the variance with corresponding principal component $A^{(1)}(t)$ showing evident pattern of EEJ strengthening and weakening. The correlation coefficient between $I(t)$ and $A^{(1)}(t)$ is around 0.49. This may confirm the linkage in some sense (only EOF-1 considered) between the positive (negative) IOD events and the weakening (strengthening) of the EEJ. The dipole pattern of lag-correlation between the sea surface temperature anomaly and U confirms the connection between the EEJ weakening/strengthening and the IOD events.

Keywords:
· Eastward equatorial jet,
· empirical orthogonal function,
· Indian Ocean dipole,
· optimal spectral decomposition,
· OSCAR data,
· dipole pattern of lag-correlation.

1. Introduction

The Indian Ocean contributes significantly to the global redistribution of heat, which is necessary to maintain the earth's thermal equilibrium. A narrow (about 500 km wide), wind-driven, high-speed (often >64 cm/s) surface jet (symmetric to the equator) flows along the equator from west to east across the entire Indian Ocean during the transition periods between the two monsoons. It appears in April and May, and again in September and October, at which times the countercurrents shift from one hemisphere to the other (Wyrtki, 1973). The sea level in the eastern Indian was unusually low, the thermocline and the mixed layer were shallow, and the subsurface flow remained eastward throughout the year. Anomalies of sea surface temperature (SST) and sea level in the eastern Indian Ocean were enhanced by upwelling favorable winds along the coast of Indonesia.

The term Indian Ocean dipole (IOD) was introduced as a basin-wide ocean-atmosphere coupled mode by Saji *et al*. (1999), Vinayachandran *et al*. (1999) and Rao *et al*. (2002). The positive IOD event is characterized by the strong positive sea surface temperature (SST) anomalies (SSTA, relative to mean SST) in the tropical western Indian Ocean (50°E–70°E, 10°S–10°N, defined as Region A) and the negative SSTA in the southeastern Indian Ocean (90°E–110°E, 10°S-equator, defined as Region B). During negative IOD events, a cold SSTA occurs in the western equatorial Indian Ocean and a warm SSTA appears in the eastern equatorial Indian Ocean, which causes a westerly wind anomaly, and in turn enhances the east-

* E-mail address: pcchu@nps.edu

ward equatorial jet (EEJ). During positive IOD events, a warm SSTA occurs in the western equatorial Indian Ocean and a cold SSTA appears in the eastern equatorial Indian Ocean, which causes an easterly wind anomaly, and in turn weakens the EEJ.

For this air-ocean coupled system, the relationship between SSTA and surface winds has been investigated thoroughly by such scientists as Yamagata *et al*. (2004) and Chang *et al*. (2006). The relationship between EEJ and SSTA has not been investigated, however. Some work using numerical model reported EEJ weakening during positive IOD events (Vinayachandran *et al*., 1999). No research has been done on the relationship among IOD events, EEJ and SSTA using long term observational data, especially the surface current velocity data. To fill this gap, we have used independent datasets (1993–2007) for this study: (a) 5-day Ocean Surface Current Analyses-Realtime (OSCAR) data from the website: http://www.oscar.noaa.gov/ mainly from satellite altimetry, (b) dipole mode index $I(t)$ from the website: http://ioc-goos-oopc.org/, and (c) SST data from the website: http://www.esrl.noaa.gov/psd/data/gridded/data.noaa.oisst.v2.html.

The remainder of the paper is organized as follows. Section 2 describes the OSCAR data and presents the annual mean (1993–2007) surface velocity field and streamfunction calculated from the reconstructed data. Section 3 depicts basic features of the surface circulation from the reconstructed OSCAR data, and demonstrates the link between the positive (negative) IOD events to the weakening (strengthening) of the EEJ. Section 4 presents the conclusions.

2. OSCAR Data and Reconstruction

The OSCAR data access system provides global data (60°S to 60°N) of operational ocean surface velocity fields on 1° × 1° grid to a broad-based user community via a web-based interactive data selection interface on a time base with exactly 72 steps per year (about 5 day spacing) starting from October 1992. The velocity is automatically computed from gridded fields of surface topography and wind derived from satellite altimeter and scatterometer vector wind data.

As Johnson *et al*. (2007) pointed out, the OSCAR data has limitations at and near the equator if one compares OSCAR satellite-derived sea surface currents with in situ data from moored current meters, drifters, and shipboard current profilers. OSCAR provides reasonably accurate temporal variability of zonal currents at periods as short as 40 days and meridional wavelengths as short as 8°. At latitudes higher than 10° the zonal current correlation remains respectable, but OSCAR amplitudes diminish unrealistically. The variability of meridional currents is poorly reproduced. Since the purpose of this study is to indentify the relationship between the narrow zonal current near the equator (i.e., EEJ) and the Indian Ocean dipole, the limitations of OSCAR data should not be too severe to our analysis.

However, since there is no lateral boundary constraint for the calculation, the OSCAR data do not show the existence of boundary currents such as the Eastern African Coastal Current (EACC), and the Somali Current. To overcome this weakness, a recently developed Optimal Spectral Decomposition method (Chu *et al*., 2003a, 2003b, 2004) was used to reconstruct the OSCAR data at each time instance, which is represented by $\mathbf{V}(x, y, t)$, where (x, y) are horizontal coordinates, and t is time.

3. Basic Features of Surface Circulation

3.1 Seasonal cycle

Since the interest of this study is to find the link between the $I(t)$ (monthly increment) and EEJ, the monthly increment data of $\mathbf{V}$ are calculated. The independent variable t is represented by two components (τ_1, τ_2) with τ_1 denoting the time sequence in years such as τ_1 = 1992, 1993, 1994, ..., 2007, and τ_2 denoting the time sequence in months within a year such as τ_2 = 1, 2, ..., 12. The monthly mean surface velocity vector field $\hat{\mathbf{V}}(x, y, \tau_2)$ is calculated by:

$$\hat{\mathbf{V}}(x, y, \tau_2) = \frac{1}{\Delta\tau} \sum_{\tau_1} \mathbf{V}(x, y, \tau_1, \tau_2), \tag{1}$$

where $\Delta\tau_1$ = 15 (October 1992 to September 2007). Figure 1 shows the mean annual cycle of the velocity vector field $\hat{\mathbf{V}}(x, y, \tau_2)$. In the winter season, the main features are North Equatorial Current (NEC), Equatorial Counter Current, South Equatorial Current, East Indian Coastal Current, and West Indian Coastal Current (Fig. 1(a)), the summer season is characterized by the Somali Current, Southwest Monsoon Current, South Equatorial Current (Fig. 1(c)). Due to seasonal reversal of the wind on the northern part of Indian Ocean, the surface circulation differs from winter to summer. From November to March (northeast monsoon), the winds blow from the southwest. The change of wind direction north of the equator then results in a change of surface current.

3.2 Surface equatorial zonal current

Zonal velocity averaged between 1°S–1°N, $u(x, t)$, is used to represent the equatorial zonal current. Time-longitude cross-section of $u(x, t)$ shows the occurrence and strength of EEJ from 1993 to 2007 (Fig. 2). Normally the EEJ lies between 60°–90°E with a speed in the range of 100–125 cm/s. It develops during April, reaches its peak intensity in May and decays by June. It re-appears

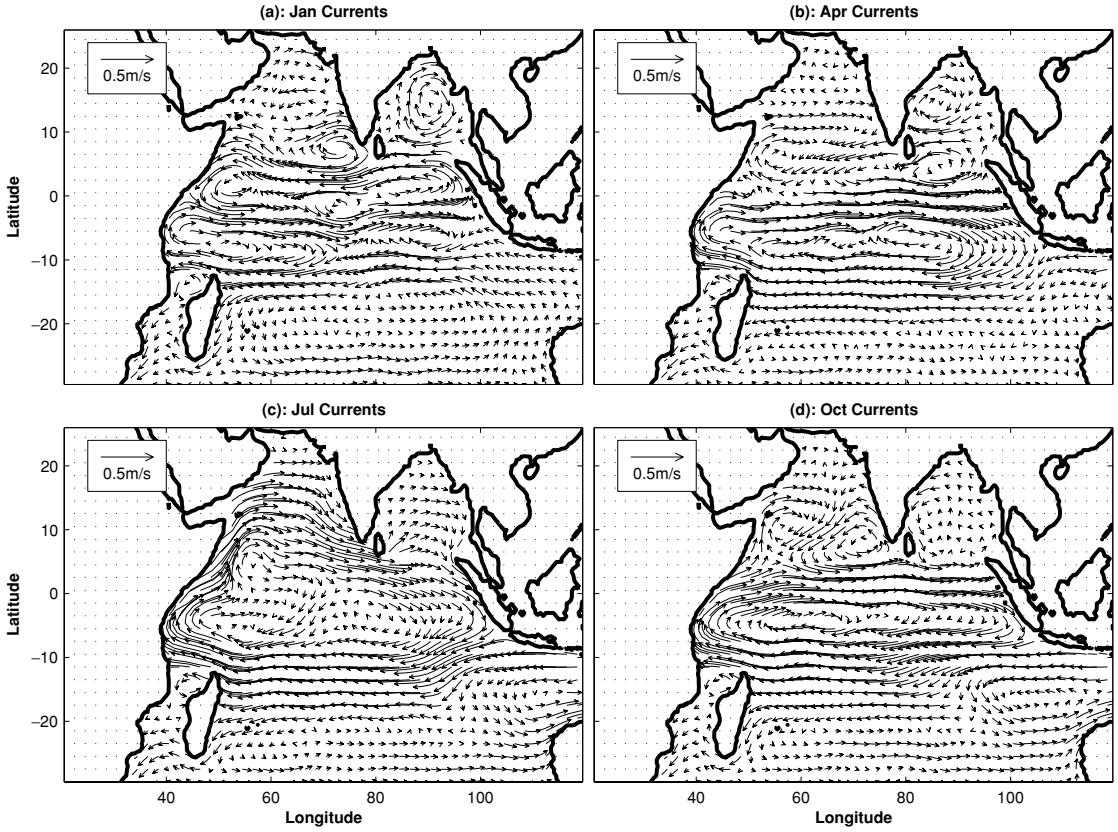

Fig. 1. (a) January, (b) April, (c) July, and (d) October mean surface velocity vectors calculated from reconstructed OSCAR data (1993–2007).

in September and October. The jets are weak during positive IOD events (1994, May 1997 to April 1998, 2006, and 2007) and strong during negative IOD events. A strong anomaly is seen during 1994, and 1997. In 1994, the speed of the spring jet was less than half its normal value and it extended eastward only up to 80°E. An eastward flow that developed east of 80°E during March was quite different from other years and was not comparable with the jet. The fall jet was absent during October 1994 and the flow east of about 70°E remained westward. Though a weak jet with a maximum speed of about 50 cm/s developed during November, its spatial and temporal extent was much shorter than other years.

An averaged zonal current over the narrow strip (42°E–100°E, 1°S–1°N) from the reconstructed OSCAR data (U) is used to represent the strength and direction of the equatorial current. Figure 3 shows the time series of 5-day U (solid curve) and monthly DMI index (dashed curve). Positive IOD events (1994, 1997, 2006, 2007) correspond to negative U (westward equatorial current), and negative IOD events (1995, 1999, 2005) correspond to positive U (eastward equatorial current). Such a connection can be explained as follows. The principal force driving the surface currents in the tropical Indian Ocean is the wind stress. The Coriolis parameter is zero at the equator so the current direction there tends to be down wind. During the positive IOD event, strong positive SSTA in the tropical western Indian Ocean, the zonal temperature gradient near the equator generates easterly winds, which in turn drive the westward equatorial current (negative U). During the negative IOD event, with a strong positive SSTA in the southern tropical eastern Indian Ocean, the zonal temperature gradient near the equator generates westerly winds, which in turn drive the eastward equatorial current (positive U).

It is noted that the relationship between IOD and zonal current is not simply linear. To confirm the existence of such a relationship, lag-correlation correlation coefficients between monthly SSTA (from NOAA a Earth System Research Laboratory) and U were calculated with SSTA advancing to U by one and two months (Fig. 4). The lag-correlation coefficients show an evident dipole pattern with positive (negative) correlation in eastern (western) equatorial Indian Ocean. During the positive IOD event, a strong positive SSTA occurs in the tropical western Indian Ocean and negative SSTA appears in the

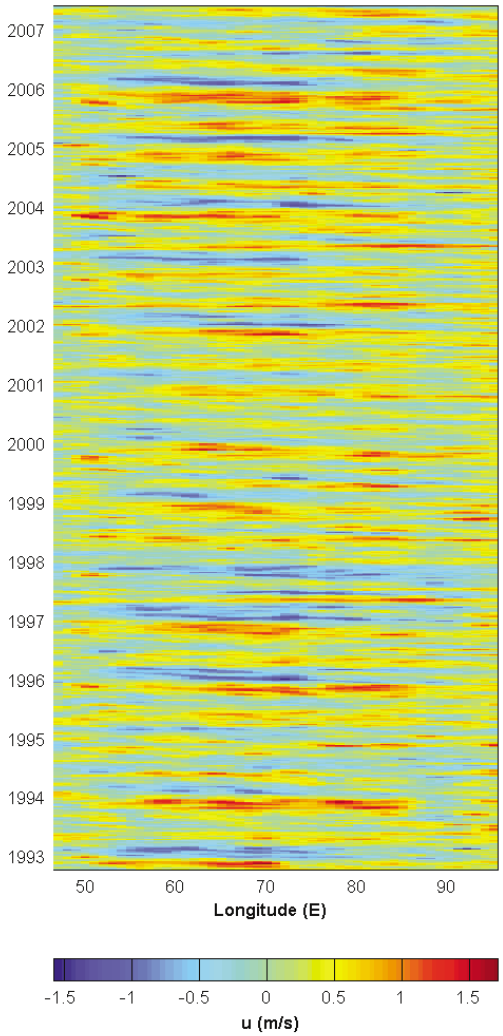

Fig. 2. Longitude-time cross-section of the equatorial zonal current (1°S–1°N).

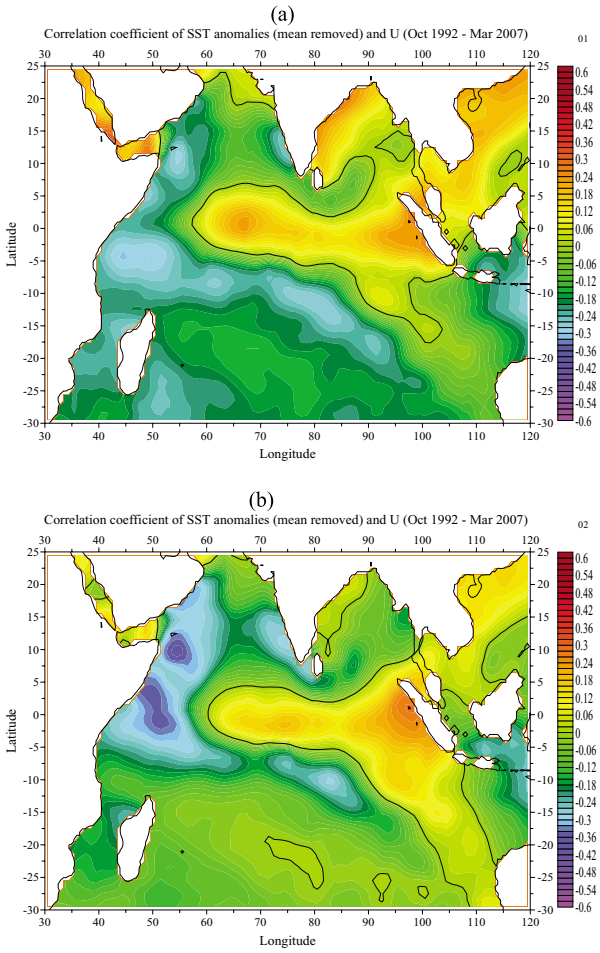

Fig. 4. Lag-correlations between monthly SSTA and mean zonal surface current (U): (a) one-month advance of SST, and (b) two-month advance of SSTA. SST data were downloaded from the NOAA Earth System Research Laboratory website: http://www.esrl.noaa.gov/psd/data/gridded/data.noaa.oisst.v2.html.

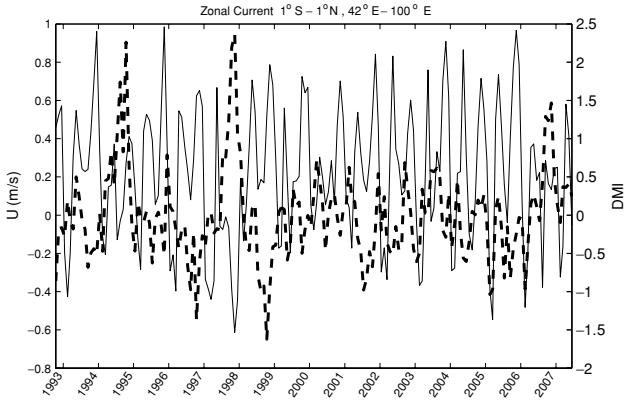

Fig. 3. Time series of 5-day mean zonal surface current (U) within the domain (1°S–1°N, 42°E–100°E) calculated from the reconstructed OSCAR data (solid curve) and monthly DMI index (dashed curve). Positive IOD events (1994, 1997, 2006, 2007) correspond to westward equatorial current (negative U), and negative IOD events (1995, 1999, 2005) correspond to eastward equatorial current (positive U).

Table 1. Variance of the first five EOFs.

EOF	Variance	Cumulative variance
1	0.5496	0.5496
2	0.2263	0.7758
3	0.0943	0.8702
4	0.0276	0.8978
5	0.0218	0.9196

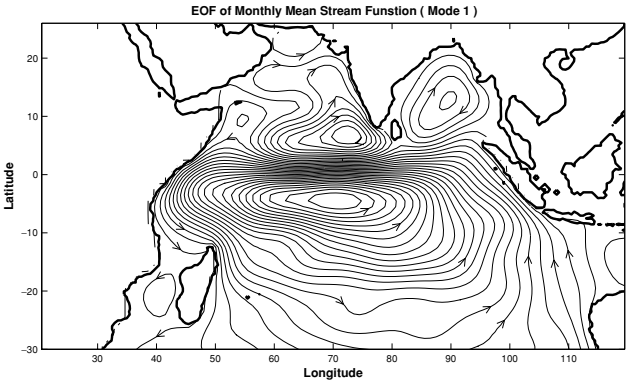

Fig. 5. EOF-1 mode $\psi_1(x, y)$ (non-dimensional).

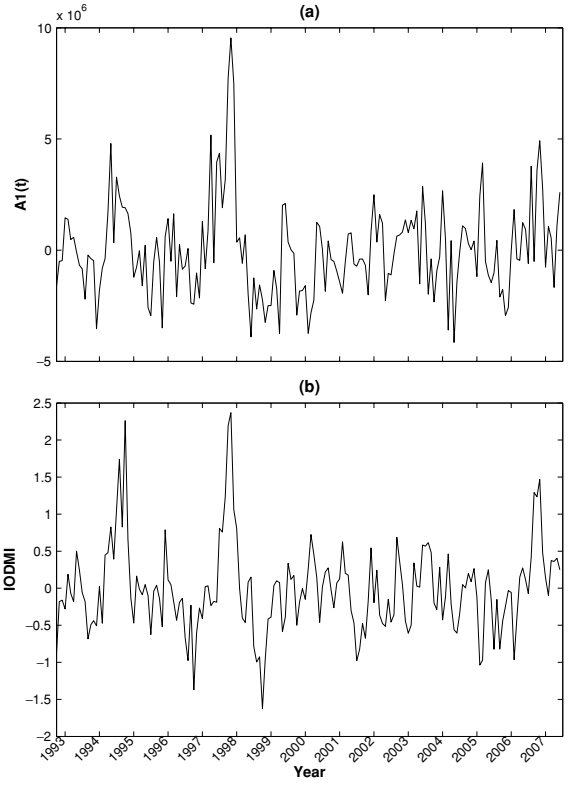

Fig. 6. Time series of (a) $A^{(1)}(t)$ (unit: m^2/s) and (b) $I(t)$.

tropical western Indian Ocean. This enhances the easterly winds and in turn causes the EEJ to weaken. Such an EEJ weakening process is also illustrated by the dipole pattern of the lag-correlation between SSTA and EEJ (Fig. 4) with negative (positive) correlation in the western (eastern) Indian Ocean. Otherwise this happens during the negative IOD event.

3.3 Non-seasonal component

The reconstructed velocity field can be decomposed into

$$\mathbf{V}(x,y,t) = \hat{\mathbf{V}}(x,y,\tau_2) + \mathbf{V}'(x,y,t),$$

where $\mathbf{V}'$ is the non-seasonal part. The corresponding streamfunction is represented by

$$\psi(x,y,t) = \hat{\psi}(x,y,\tau_2) + \psi'(x,y,t). \quad (2)$$

The EOF method is used to analyze the temporal and spatial variability of the non-seasonal streamfunction at the surface, $\psi'(x, y, t)$. The first EOF is able to account for 55% variance (Table 1),

$$\psi'(x,y,t) = A^{(1)}(t)\psi_1(x,y). \quad (3)$$

Here, $\psi_1(x, y)$ is the EOF-1 mode (non-dimensional), and $A^{(1)}(t)$ (unit: m^2s^{-1}) is the corresponding principal component. As mentioned in Subsection 3.1, the seasonal streamfunction $\hat{\psi}(x, y, \tau_2)$ shows the appearance of EEJ in spring and fall and disappearance in winter and summer. However, EOF-1 (Fig. 5) shows the opposite flow pattern (westward) in the equatorial region, which causes a weakening EEJ for positive $A^{(1)}(t)$, and a strengthening EEJ for negative $A^{(1)}(t)$ (Fig. 6(a)). The correlation coefficient between $A^{(1)}(t)$ and $U(t)$ is –0.61, which is consistent with the above argument.

The dipole mode index (DMI), represented by $I(t)$ in this study, is defined as the zonal difference of SSTA between region A and region B. The IOD is an ocean-atmosphere coupled and seasonally phase-locked phenomenon starting around April and peaking in October (e.g., Vinayachandran *et al.*, 1999; Yamagata *et al.*, 2004).

The linkage between IOD and EEJ is also represented by the correlation coefficient (0.49) between the two time series $A^{(1)}(t)$ (Fig. 6(a)) and $I(t)$ (Fig. 6(b)). The total size of the time series (n) is 180 (15 years of monthly data between 1993 and 2007). For the significance level α = 0.01, the critical value for the correlation coefficient is 0.208 (0.181) with degree of freedom 150 (200) (Emery and Thomson, 2001, p. 585). Thus, the correlation coef-

ficient (0.49) is significant between $I(t)$ and $A^{(1)}(t)$ for $\alpha = 0.01$.

4. Conclusions

Two independent observational datasets (IOD mode index and OSCAR) from October 1992 to September 2007 have been used in this study. The mean seasonal cycle of the surface circulation shows that the EEJ occurs in spring and fall. The horizontally averaged (1°S–1°N, 42°E–100°E) zonal velocity is negative (westward) during positive IOD events and positive (eastward) during negative IOD events. The first EOF mode (accounting for 55% of variance) of the streamfunction calculated from the OSCAR data shows evident weakening/strengthening of the eastward equatorial jet in both spring and fall seasons. Such a relationship is consistent with the dipole pattern of lag-correlation between monthly mean SSTA and U with 1–2 month advance of SSTA. An evident correlation between the IOD mode index and the principle component of the EOF-1 confirms the linkage between the positive (negative) IOD events and the weakening (strengthening) of the eastward equatorial jet. Since only the EOF-1 mode is used for the analysis, the results should be used with caution.

Acknowledgements

The author would like to thank Chenwu Fan and Yu-Heng Kuo for invaluable comments and computational assistance, NOAA for OSCAR and SST data, and Ocean Observations Panel for Climate for the DMI index data. The Office of Naval Research, Naval Oceanographic Office, and Naval Postgraduate School sponsored this research.

References

Chang, P., T. Yamagata, P. Schopf, S. K. Behera, J. Carton, W. S. Kessler, G. Meyers, T. Qu, F. Schott, S. Shetye and S.-P. Xie (2006): Climate fluctuations of tropical coupled systems-the role of ocean dynamics. *J. Climate*, **19**, 5122–5174.

Chu, P. C., L. M. Ivanov, T. P. Korzhova, T. M. Margolina and O. M. Melnichenko (2003a): Analysis of sparse and noisy ocean current data using flow decomposition. Part 1: Theory. *J. Atmos. Oceanic Technol.*, **20**, 478–491.

Chu, P. C., L. M. Ivanov, T. P. Korzhova, T. M. Margolina and O. M. Melnichenko (2003b): Analysis of sparse and noisy ocean current data using flow decomposition. Part 2: Application to Eulerian and Lagrangian data. *J. Atmos. Oceanic Technol.*, **20**, 492–512.

Chu, P. C., L. M. Ivanov and T. M. Margolina (2004): Rotation method for reconstructing process and field from imperfect data. *Int. J. Bifur. Chaos*, **14**, 2991–2997.

Emery, W. J. and R. E. Thomson (2001): *Data Analysis Methods in Physical Oceanography*. 2nd revised ed., Elsevier, Amsterdam, 638 pp.

Johnson, E. S., F. Bonjean, G. S. E. Lagerloef and J. T. Gunn (2007): Validation and error analysis of OSCAR sea surface currents. *J. Atmos. Oceanic Technol.*, **24**, 688–701.

Rao, A. S., S. K. Behera, Y. Masumoto and T. Yamagata (2002): Interannual variability in the subsurface tropical Indian Ocean. *Deep-Sea Res. II*, **49**, 1549–1572.

Saji, N. H., B. N. Goswami, P. N. Vinayachandran and T. Yamagata (1999): A dipole in the tropical Indian Ocean. *Nature*, **401**, 360–363.

Vinayachandran, P. N., N. H. Saji and T. Yamagata (1999): Response of the equatorial Indian Ocean to an unusual wind event during 1994. *Geophys. Res. Lett.*, **26**, 1613–1616.

Wyrtki, K. (1973): An equatorial jet in the Indian Ocean. *Science*, **181**, 262–264.

Yamagata, T., S. K. Behera, J.-J. Luo, S. Masson, M. Jury and S. A. Rao (2004): Coupled ocean-atmosphere variability in the tropical Indian Ocean. p. 189–212. In *Earth Climate: The Ocean-Atmosphere Interaction*, ed. by C. Wang, S.-P. Xie and J. A. Carton, *Geophys. Monogr.*, Vol. 147, AGU, Washington, D.C.